



First-principles calculations on the first row transition metals-substituted TMC_6N_7 clusters

Zhi Li¹ · Zhen Zhao² · Tao-tao Shao¹

Received: 31 January 2020 / Accepted: 23 March 2020 / Published online: 2 April 2020
© Springer Nature B.V. 2020

Abstract

The configurations, stabilities, electronic, and magnetic attributes of the first row transition metal (TM)-substituted TMC_6N_7 clusters have been investigated at the PBE level. The results display that the first row TM atoms are inclined to replace the N atom which approaches the N atom out of the C–N rings except for Cu and Zn. As for the CuC_6N_7 and ZnC_6N_7 clusters, the N atom out of the C–N rings is inclined to be substituted. The $\text{ScC}_6\text{N}_7(\text{GS})$, $\text{TiC}_6\text{N}_7(\text{GS})$, $\text{VC}_6\text{N}_7(\text{GS})$, $\text{CoC}_6\text{N}_7(\text{GS})$, $\text{TiC}_6\text{N}_7(\text{a})$, and $\text{CoC}_6\text{N}_7(\text{a})$ clusters display more structural stabilities than the pristine C_6N_8 clusters. The ground-state $3d$ TMC_6N_7 clusters exhibit more dynamic stabilities than the pristine C_6N_8 clusters except for Zn. Partial of $4s$ orbital electrons of TM atoms is transferred to the neighbor C atoms. The V, Cr, Mn, and Fe atoms of the ground-state TMC_6N_7 clusters display the opposite spin to Co and Ni atoms of the ground-state TMC_6N_7 clusters.

Keywords C_6N_8 clusters · First-principles · Electronic properties · Magnetic properties

Introduction

Graphite carbon nitride ($\text{g-C}_3\text{N}_4$) has been regarded as an excellent carbon carrier of catalyst [1]. It has the advantages of low cost, simple synthesis, thermal and chemical stabilities, biocompatibility, and non-toxicity, etc. [2–5]. However, the photocatalytic efficiency of pristine $\text{g-C}_3\text{N}_4$ is limited by the intrinsic lack of light-absorbance, charge mobility, and recombination rate of electron–hole pairs [6]. To solve these problems, doping has been widely adopted to modulate the electronic

✉ Zhi Li
lizhi81723700@163.com

¹ School of Materials and Metallurgy, University of Science and Technology Liaoning, Anshan 114051, People's Republic of China

² School of Chemistry and Life Science, Anshan Normal University, Anshan 114007, People's Republic of China

configurations of $g\text{-C}_3\text{N}_4$ to improve conductivity, optics, magnetism, etc. [7]. That is, doping reduces electronic transition energy and provides a ‘bridge’ for lower energy photo-generated electrons [3]. Various non-metals and metals have been considered to modify the intrinsic characteristics and obtain novel properties of layered $g\text{-C}_3\text{N}_4$ [8]. $g\text{-C}_3\text{N}_4$, with rich pyridine-like nitrogen, prefers to trap TM atoms to the hexagonal rings of $g\text{-C}_3\text{N}_4$ [1, 3]. At present, a large number of studies have been performed on first row TM (i.e., Ti [9], V [10], Cr [4], Mn [1, 8, 11], Fe [1, 7, 11–18], Co [1, 11, 14, 16, 19], Ni [20], Cu [11, 12, 16, 21, 22], and Zn [11, 17, 23]) doping on the $g\text{-C}_3\text{N}_4$ sheet. The strong hybridization between $3d$ orbitals of TM atoms and the p_π orbitals of $g\text{-C}_3\text{N}_4$ not only can improve the photocatalytic properties but also can induce spin polarization [1, 3, 8]. Given the complexity of the reaction process, we have calculated the $3d$ TM-substituted TMC_5N_8 clusters [24]. However, the difference in the radius of C (0.86 nm) and N (0.80 nm) atoms is so small [3]. The precise recognition of the effective active sites has not been explored [25]. $gh\text{-C}_3\text{N}_4$ is more stable than $gt\text{-C}_3\text{N}_4$ [8], and the structural unit of $g\text{-C}_3\text{N}_4$ is ordered tri-*s*-triazine (C_6N_7) which is planar and aromatic [26]. C_6N_7 can provide many binding sites that interact with metals or other pollutants [18].

C_3N_4 exhibits versatile electronic and magnetic properties which originate from the hole geometrical character [27, 28]. In this study, the configurations, stabilities, electronic, and magnetic properties of the TMC_6N_7 clusters are investigated by using density functional theory (DFT). It is very important to understand the evolution mechanisms of $gh\text{-C}_3\text{N}_4$ -based materials. It is also helpful to control defects and design novel properties of C_3N_4 -based materials [28].

Computational details

The pristine C_6N_8 clusters are extracted by $gh\text{-C}_3\text{N}_4$ in Ref. [8]. A TM atom is adopted to substitute a N atom of the pristine C_6N_8 clusters in order to design the TMC_6N_7 clusters, respectively. The optimization and property calculations have been performed by DFT which are implemented in the DMol³ package. The Perdew–Burke–Ernzerhof (PBE) functional (including a semi-empirical van der Waals (vdW) correction) within the generalized gradient approximation (GGA) is adopted for the exchange–correlation [26, 29]. Because of strong electronic coupling of TM atoms of the TMC_6N_7 clusters [30], the approximate semi-classical dispersion correction scheme DFT+D must be selected [31, 32]. In order to avoid omitting certain configurations of the TMC_6N_7 clusters, symmetry unconstraints is adopted [33, 34]. Considering the electron relativity effects of the TM atoms, all electron relativistic treatment is selected [35]. Spin polarized is selected as a result of certain TM atoms exhibit high spins [34]. Double numerical plus polarization (DNP) is used [32, 36]. Furthermore, the Mülliken population analysis is executed to obtain the net charges and spin properties of the TMC_6N_7 clusters [34].

The average binding energy (E_b) of the TMC_6N_7 clusters was calculated to determine the structural stability [34]:

$$E_b = [E(\text{TM}) + 6E(\text{C}) + 7E(\text{N}) - E(\text{TMC}_6\text{N}_7)]/14 \quad (1)$$

where $E(\text{TM})$, $E(\text{C})$, and $E(\text{N})$ present the total energies of isolated TM, C, and N atoms, respectively. $E(\text{TMC}_6\text{N}_7)$ is the total energy of the TMC_6N_7 clusters.

In order to determine the accuracy of the PBE functional selected, the calculated distance (6.840 Å) between two nitride pores is compared with the corresponding experimental value (6.81 Å) [37]. And the calculated lattice constant (7.138 Å) of $\text{gh-C}_3\text{N}_4$ agree well with the other computational results (7.13 Å [38] and 7.14 Å [39]) and the experimental value (7.13 Å [40]). As for the TM atom doping, it has been confirmed in our previous work [35]. Consequently, the PBE functional is selected to investigate the TMC_6N_7 clusters.

Results and discussion

Configurations

The optimized configurations of the TMC_6N_7 clusters have been displayed in Fig. 1. The gray balls present C atoms, the blue balls present N atoms, and other balls present TM atoms, respectively. Owing to the radius of TM atoms is larger generally than the substituted N atoms. It leads to the symmetry of the pristine C_6N_8 clusters is degraded to C_1 . The unplanar structures of the TMC_6N_7 clusters in Fig. 1 are labeled a star (*). As for these unplanar TMC_6N_7 clusters, the pseudo-Jahn–Teller distortion due to the electronic coupling of TM atoms leads to the planar C_6N_8 clusters is transformed into the characteristic buckling [41]. And TM atoms will advance the transformation from the quasi-planar configurations to three-dimensional structures [42]. As for the planar

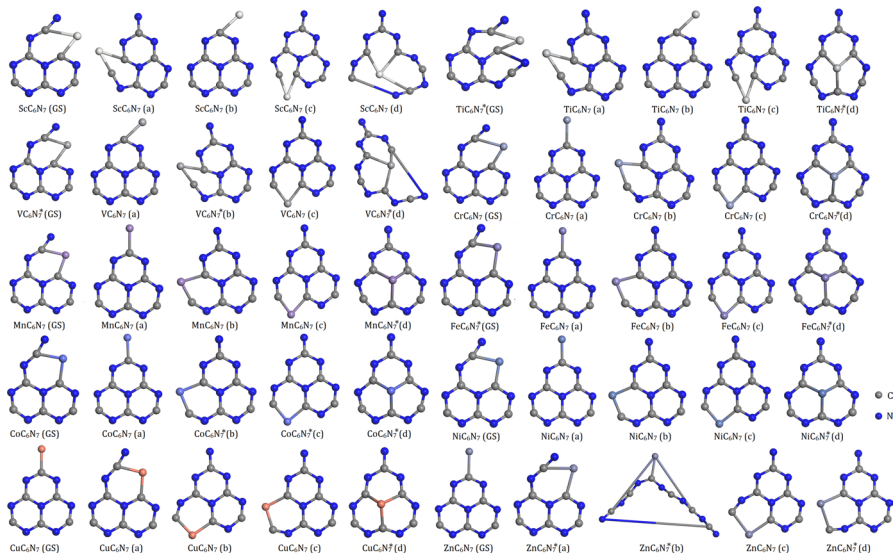


Fig. 1 Configurations of the TMC_6N_7 clusters

TMC₆N₇ clusters which have not yield any significant distortion, it suggests that the interaction between them is weaker [43]. 3d atoms are inclined to replace the N atom which approaches the N atom out of the C–N rings except for Cu and Zn. As for the CuC₆N₇ and ZnC₆N₇ clusters, the N atom out of the C–N rings is inclined to be substituted. It derives from the polarization of Cu⁺ ion and Zn²⁺ ion is stronger than that of other 3d TM atoms according to electron configurations, which leads to the prominent polarization between them and the C₆N₇ fragments, and the corresponding chemical bonds transition from ionic bonds to covalent bonds. The isomers (d) which the N atoms in the centre of C–N rings substituted except for ZnC₆N₇(d) are the most unstable structures. It originates from a larger effective decay radius of Zn which indicates a more intense localization of impurity states [43]. Wang et al. [2] have observed the pore size of the Zn-doped C₃N₄ sheet expands by the BET analysis. The ZnC₆N₇(b) clusters become a typical. Even it is more exaggerating than the ZnC₅N₈(c) clusters [24]. And Yue et al. [23] have confirmed that Zn doping partly damages the structure of g-C₃N₄. Nevertheless, cross-link effect of Zn between the interlayers of g-C₃N₄ sheet is helpful to obstruct the exfoliation of g-C₃N₄ [2]. However, Zn doping will create active sites on the surface of g-C₃N₄ for reducing protons into H₂ [44].

Stabilities

The average binding energies E_b of the TMC₆N₇ clusters have been displayed in Fig. 2. The first row TM symbols are listed to expound the abscissa of Figs. 2, 3, 4, 5. The negative value of the binding energy presents a stable doping system [3]. ScC₆N₇(GS), TiC₆N₇(GS), VC₆N₇(GS), CoC₆N₇(GS), TiC₆N₇(a), and CoC₆N₇(a) actually improve the structural stabilities of the C₆N₈ clusters. As for other 3d TM atoms, they prefer to segregate and then aggregate the TM clusters [26]. In our previous work, only ScC₅N₈(GS), TiC₅N₈(GS), and VC₅N₈(GS) can increase the structural stabilities of the pristine C₆N₈ clusters [24]. Xiong et al. [45] have confirmed Ti doping can improve the thermodynamic stabilities of the CN_x coatings.

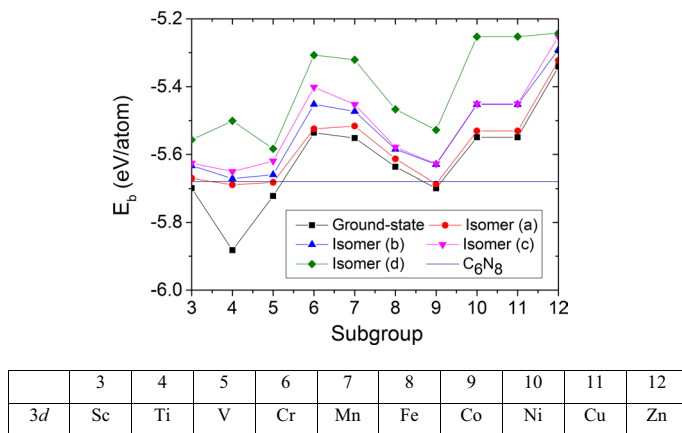


Fig. 2 Average binding energies of the TMC₆N₇ clusters

Fig. 3 HOMO–LUMO gaps of the TMC_6N_7 clusters

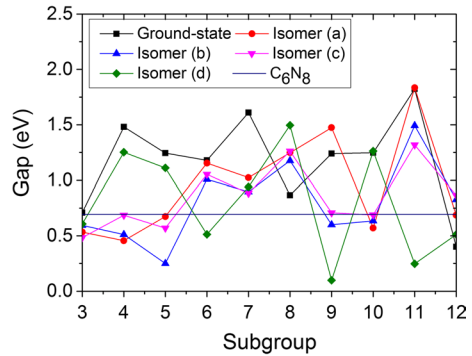


Fig. 4 Net charges of the TM atoms in the TMC_6N_7 clusters

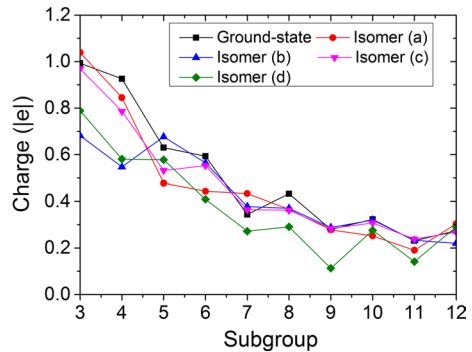
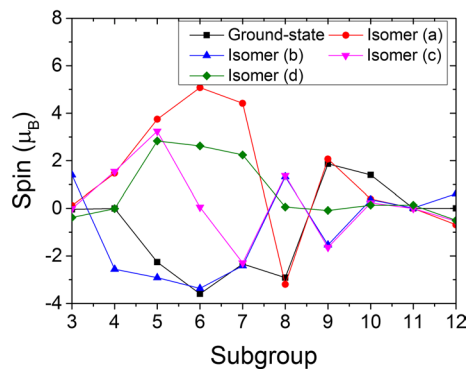


Fig. 5 Spins of the TM atoms in the TMC_6N_7 clusters



The energy gaps between the highest occupied molecular orbital (HOMO) states and the lowest unoccupied molecular orbital (LUMO) states of the TMC_6N_7 clusters have been plotted in Fig. 3. Although the calculated HOMO–LUMO gap (0.694 eV) of the pristine C_6N_8 clusters is significantly narrower than the experimental value (2.7 eV) of C_3N_4 [4], it seems to be confirmed by that (1.24 eV) of monolayer CN [38] and that (1.22 eV) of two-dimensional C_6N_8 [28], and that (1.040 eV) of the sole g- C_3N_4 [29]. The HOMO–LUMO gaps of the ground-state TMC_6N_7 clusters as an example, the TM substituting can improve the dynamic stabilities of the pristine C_6N_8 clusters except for

Zn. It is significantly different from those of the TMC_5N_8 clusters [24]. It originates from the hybridization between d orbitals of the TM atoms and p orbitals of the neighbor C atoms in the TMC_6N_7 clusters which is less than that between d - p orbitals of TM and N atoms of the TMC_5N_8 clusters [24, 26]. The metallic properties of Zn at the top site of the ZnC_6N_7 clusters are better kept because of Zn atoms exhibit the all paired $3d^{10}$ orbital systems [26]. The metal-like electronic density of states of Zn will increase the non-adiabatic instability of the pristine C_6N_8 clusters [46].

To expound the influence of TM atom substituted the pristine C_6N_8 clusters, the HOMO and LUMO states of the ground-state TMC_6N_7 clusters have been displayed in Table 1. The blue regions prefer to trap electrons, and the yellow regions prefer to

Table 1 HOMO and LUMO orbitals of the ground-state TMC_6N_7 clusters

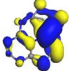
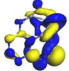
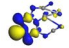
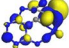
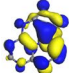
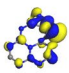
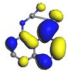
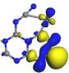


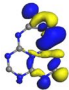
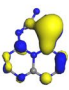
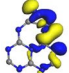
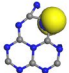
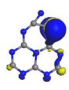
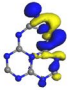
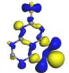
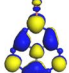
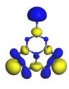
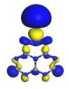
Cluster	HOMO	LUMO
ScC_6N_7		
TiC_6N_7		
VC_6N_7		
CrC_6N_7		
MnC_6N_7		
FeC_6N_7		
CoC_6N_7		
NiC_6N_7		
CuC_6N_7		
ZnC_6N_7		

Table 2 Mulliken charges Q (unit: |e|) of the C_6N_8 and the ground-state TMC_6N_7 clusters

	C_6N_8	ScC_6N_7	TiC_6N_7	VC_6N_7	CrC_6N_7	MnC_6N_7	FeC_6N_7	CoC_6N_7	NiC_6N_7	CuC_6N_7	ZnC_6N_7
Q_1	-0.202	-0.507	-0.492	-0.410	-0.419	-0.362	-0.374	-0.349	-0.353	0.256	0.306
Q_2	-0.262	-0.276	-0.312	-0.218	-0.227	-0.250	-0.230	-0.216	-0.209	-0.237	-0.243
Q_3	0.329	0.329	0.351	0.302	0.356	0.354	0.269	0.315	0.289	0.050	0.032
Q_4	-0.262	1.021	0.949	0.653	0.613	0.369	0.458	0.311	0.345	-0.237	-0.244
Q_5	-0.227	-0.299	-0.282	-0.247	-0.269	-0.262	-0.248	-0.244	-0.246	-0.254	-0.241
Q_6	0.447	0.455	0.416	0.398	0.419	0.444	0.458	0.446	0.452	0.426	0.434
Q_7	-0.507	-0.438	-0.382	-0.380	-0.423	-0.445	-0.465	-0.457	-0.447	-0.431	-0.425
Q_8	0.448	-0.026	-0.231	0.054	0.051	0.194	0.081	0.143	0.106	0.426	0.434
Q_9	-0.228	-0.435	-0.466	-0.329	-0.293	-0.318	-0.272	-0.277	-0.280	-0.254	-0.241
Q_{10}	0.257	0.185	0.182	0.159	0.170	0.185	0.186	0.178	0.181	0.171	0.127
Q_{11}	-0.275	-0.292	-0.281	-0.243	-0.264	-0.272	-0.264	-0.255	-0.254	-0.257	-0.247
Q_{12}	0.489	0.448	0.439	0.390	0.413	0.447	0.460	0.452	0.454	0.430	0.430
Q_{13}	-0.273	-0.313	-0.270	-0.256	-0.271	-0.265	-0.249	-0.232	-0.230	-0.257	-0.247
Q_{14}	0.265	0.150	0.378	0.129	0.143	0.181	0.191	0.186	0.191	0.171	0.126

release electrons [47]. The total charge density displays a high charge density around the TM atoms [47, 48], projecting to the C-TM bonds, indicating charge transfer from TM to C atoms. The degree of charge redistribution is mainly proportional to the interaction strength [48]. As for the ground-state TMC_6N_7 clusters except for the ZnC_6N_7 clusters, the HOMO and LUMO states display the hybridization between the $3d$ orbital electrons of the TM atoms and the $2p$ orbital electrons of the C atoms. While for the ground-state ZnC_6N_7 clusters, the hybridization effect is limited because of the Zn atoms exhibit the all paired $3d^{10}$ orbital systems [26].

Electronic properties

The net charges of the TM atoms of the TMC_6N_7 clusters have been plotted in Fig. 4. The positive charges on the TM atoms decrease generally as atomic number of the TM atoms increasing which is similar to that on TM embedded the sole $\text{g-C}_3\text{N}_4$ [29]. As for the ground-state TMC_6N_7 clusters, the TM atoms loss a few electrons within the scope of 0.113 |e| and 1.039 |e|. As for the transferred charge amounts of TM atoms of the TMC_6N_7 clusters are generally less than those (from 0.375|e| to 1.150|e|) of TM atoms of the TMC_5N_8 clusters [24]. It derives from the TM atoms and the neighbor C atoms of the TMC_6N_7 clusters prefer to the electropositive which is different from that of the TM atoms and the neighbor negative N atoms of the TMC_5N_8 clusters [48]. Z. Zhu et al. [38] have confirmed that the charge transfer of Co and $\text{g-C}_3\text{N}_4$ by Raman enhancement factors. The electron transfer follows the formation of chemical bonds [49]. The covalent bonding character of TM-C of TM-adsorbed BC_6N have been confirmed [43]. The differences in the net charges of TM atoms of the TMC_6N_7 isomers are shown in Fig. 4 and the Mülliken charges of the C and N atoms of the TMC_6N_7 clusters are given in Table 2. (The Mülliken charges in Table 2 have been listed by the order from top to bottom and from left to right of atoms of the TMC_6N_7 isomers in Fig. 1.) It originates from the different atomic arrangements [50].

The natural electron configurations of the ground-state TMC_6N_7 clusters have been listed in Table 3. Compare the natural electron configurations of isolated TM atoms with those of the TM atoms of the TMC_6N_7 clusters in Table 3, the $4s$ orbital of the TM atoms of the TMC_6N_7 clusters lose more electrons than the $3d$ and $4p$ orbitals of the obtained. It confirms the hybridization mechanism of the sp orbital electrons of the TMC_6N_7 clusters.

Magnetic properties

The spins of TM atoms of the TMC_6N_7 clusters have been displayed in Fig. 5. The spins of the TM atoms of the TMC_6N_7 clusters are found to be lower than those of isolated TM atoms in Ref. [35], it originates from the certain d orbital electrons are transferred or magnetic couplings in the TMC_6N_7 clusters [26, 48]. As for the ground-state TMC_6N_7 clusters, the maximum spins of the TM atoms appear at Cr

Table 3 Natural electron configurations of the TM atoms in the ground-state TMC_6N_7 clusters

Cluster	Atom	Natural electron configuration
ScC_6N_7	Sc	[core]3d(1.610)4s(0.216)4p(0.181)
TiC_6N_7	Ti	[core]3d(2.579)4s(0.204)4p(0.301)
VC_6N_7	V	[core]3d(3.742)4s(0.340)4p(0.277)
CrC_6N_7	Cr	[core]3d(4.786)4s(0.359)4p(0.282)
MnC_6N_7	Mn	[core]3d(5.857)4s(0.447)4p(0.335)
FeC_6N_7	Fe	[core]3d(6.705)4s(0.508)4p(0.342)
CoC_6N_7	Co	[core]3d(7.793)4s(0.524)4p(0.388)
NiC_6N_7	Ni	[core]3d(8.785)4s(0.559)4p(0.323)
CuC_6N_7	Cu	[core]3d(9.745)4s(0.934)4p(0.096)
ZnC_6N_7	Zn	[core]3d(9.990)4s(1.471)4p(0.265)

and Fe. It derives from the 3d orbitals of Cr which display strong spin exchange splitting ε_d [51]. The V, Cr, and Fe atoms doping the g- C_3N_4 display ferromagnetic states [26], while Mn exhibits an anti-ferromagnetic behavior [26, 52]. While for Cu and Zn atoms of the TMC_6N_7 clusters display the nonmagnetic states because of the all paired d orbital structures [26]. The Cu and Zn atoms of TM-g- C_3N_4 sheets display nonmagnetic which has been confirmed [26]. As for the discrete spins of the TMC_6N_7 isomers, it derives from the spatial arrangements of interacting magnetic orbitals [26]. The neighboring C_{edge} atoms exhibit oppositely spin polarized with respect to the TM atoms [8].

Conclusions

In summary, the configurations, stabilities, electronic, and magnetic attributes of the first row transition metal (TM)-substituted TMC_6N_7 clusters have been investigated at the PBE level. The results display that the 3d TM atoms are inclined to replace the N atom which approaches the N atom out of the C-N rings except for Cu and Zn. As for the CuC_6N_7 and ZnC_6N_7 clusters, the N atom out of the C-N rings prefers to be substituted. The $\text{ScC}_6\text{N}_7(\text{GS})$, $\text{TiC}_6\text{N}_7(\text{GS})$, $\text{VC}_6\text{N}_7(\text{GS})$, $\text{CoC}_6\text{N}_7(\text{GS})$, $\text{TiC}_6\text{N}_7(\text{a})$, and $\text{CoC}_6\text{N}_7(\text{a})$ clusters display more structural stabilities than the C_6N_8 clusters. The ground-state 3d TMC_6N_7 clusters exhibit more dynamic stabilities than the C_6N_8 clusters except for Zn. A small amount of 4s orbital electrons of the TM atoms is transferred to the neighbor C atoms by the net charge distribution of the TMC_6N_7 clusters. The V, Cr, Mn, and Fe atoms of the ground-state TMC_6N_7 clusters display the opposite spin to Co and Ni atoms of the ground-state TMC_6N_7 clusters.

Acknowledgements We gratefully acknowledge the financial support from the Key Fund Project of the National Science Foundation, People's Republic of China (Grant No. 51634004), Key Laboratory of Chemical Metallurgy Engineering Liaoning Province, University of Science and Technology Liaoning (Grant No. USTLKFYSY201711) and the Fund Project of University of Science and Technology Liaoning (Grant No. 2017YY02).

References

1. Q. Liu, J.Y. Zhang, *Langmuir* **29**, 3821 (2013)
2. Z.T. Wang, J.L. Xu, H. Zhou, X. Zhang, *Rare Met.* **38**, 459 (2019)
3. R. Zhang, S. Niu, X. Zhang, Z. Jiang, J. Zheng, C. Guo, *Appl. Surf. Sci.* **489**, 427 (2019)
4. Y. Zhang, Q. Zhang, Q. Shi, Z. Cai, Z. Yang, *Sep. Purif. Technol.* **142**, 251 (2015)
5. H.A. Bicalho, J.L. Lopez, I. Binatti, P.F.R. Batista, J.D. Ardisson, R.R. Resende, E. Lorencon, *Mol. Catal.* **435**, 156 (2017)
6. C. Sun, H. Zhang, H. Liu, X. Zheng, W. Zou, L. Dong, L. Qi, *Appl. Catal. B Environ.* **235**, 66 (2018)
7. J. Gao, Y. Wang, S. Zhou, W. Lin, Y. Kong, *ChemCatChem* **9**, 1708 (2017)
8. D. Ghosh, G. Periyasamy, B. Pandey, S.K. Pati, *J. Mater. Chem.* **2**, 7943 (2014)
9. Y. Wang, Y. Wang, Y. Chen, C. Yin, Y. Zuo, L.-F. Cui, *Mater. Lett.* **139**, 70 (2015)
10. G.D. Ding, W.T. Wang, T. Jiang, B.X. Han, H.L. Fan, G.Y. Yang, *Chemcatchem* **5**, 192 (2013)
11. Z. Ding, X. Chen, M. Antonietti, X. Wang, *Chemsuschem* **4**, 274 (2011)
12. Z. Li, C. Kong, G. Lu, *J. Phys. Chem. C* **120**, 56 (2016)
13. J. Ma, Q. Yang, Y. Wen, W. Liu, *Appl. Catal. B: Environ.* **201**, 232 (2017)
14. X. Chen, J. Zhang, X. Fu, M. Antonietti, X. Wang, *J. Am. Chem. Soc.* **131**, 11658 (2009)
15. S. Tonda, S. Kumar, S. Kandula, V. Shanker, *J. Mater. Chem. A* **2**, 6772 (2014)
16. W. Oh, V.W.C. Chang, Z. Hu, R. Goei, T. Lim, *Chem. Eng. J.* **323**, 260 (2017)
17. X.C. Wang, X.F. Chen, A. Thomas, X.Z. Fu, M. Antonietti, *Adv. Mater.* **21**, 1609 (2009)
18. Q. Liao, D. Zou, W. Pan, W. Linghu, R. Shen, Y. Jin, G. Feng, X. Li, F. Ye, A.M. Asiri, H.M. Marwani, Y. Zhu, X. Wu, W. Dong, *J. Mol. Liq.* **258**, 275 (2018)
19. L. Deng, M. Zhu, *RSC Adv.* **6**, 25670 (2016)
20. L. Kong, Y. Dong, P. Jiang, G. Wang, H. Zhang, N. Zhao, *J. Mater. Chem. A* **4**, 9998 (2016)
21. B. Tahir, M. Tahir, N.A.S. Amin, *Appl. Surf. Sci.* **419**, 875 (2017)
22. M. Ji, J. Huang, K. Zhang, D. He, S. Chang, D. Luo, E. Zhang, M. Xu, J. Liu, J. Zhang, J. Xu, J. Wang, *C. Zhu, Inorg. Chem. Front.* **5**, 2420 (2018)
23. B. Yue, Q. Li, H. Iwai, T. Kako, J. Ye, *Sci. Technol. Adv. Mater.* **12**, 034401 (2011)
24. Z. Li, Z. Zhao, Z. Liu, H. Wang, Q. Wang, *Res. Chem. Intermediat.* **46**, 2099 (2020)
25. S. Sarkar, S.S. Sumukh, K. Roy, N. Kamboj, T. Purkait, M. Das, R. Sundar Dey, *J. Colloid Interf. Sci.* **558**, 182 (2019)
26. E. Kroke, *Angew. Chem. Int. Edit.* **53**, 11134 (2014)
27. A. Bafekry, C. Stampfl, S. Farjami Shayesteh, *ChemPhysChem* **21**, 164 (2020)
28. A. Bafekry, S. Farjami Shayesteh, F.M. Peeters, *J. Appl. Phys.* **126**, 215104 (2019)
29. T. Wang, G. Yu, J. Liu, X. Huang, W. Chen, *Phys. Chem. Chem. Phys.* **21**, 1773 (2019)
30. Y. Yang, C. Yin, K. Li, H. Tang, Y. Wang, Z. Wu, *J. Electrochem. Soc.* **166**, F755 (2019)
31. S.A. Khandy, D.C. Gupta, *RSC Adv.* **6**, 48009 (2016)
32. Y. Guo, C. Tang, X. Wang, C. Wang, L. Fu, *Chin. Phys. B* **28**, 048102 (2019)
33. Z. Zhao, Z. Li, Q. Wang, T. Shi, *Mater. Chem. Phys.* **240**, 122220 (2020)
34. Z. Zhao, Z. Li, *Mod. Phys. Lett. B* **33**, 1950459 (2019)
35. Z. Zhao, Z. Li, Q. Wang, *Chem. Phys. Lett.* **739**, 136922 (2020)
36. B. Delley, *J. Chem. Phys.* **113**, 7756 (2000)
37. X. Wang, K. Maeda, A. Thomas, K. Takanabe, G. Xin, J.M. Carlsson, K. Domen, M. Antonietti, *Nat. Mater.* **8**, 76 (2009)
38. Z. Zhu, X. Tang, T. Wang, W. Fan, Z. Liu, C. Li, P. Huo, Y. Yan, *Appl. Catal. B Environ.* **241**, 319 (2018)
39. J. Cui, S. Liang, X. Wang, J. Zhang, *J. Mater. Chem. Phys.* **161**, 194 (2015)
40. P. Niu, L. Zhang, G. Liu, *Adv. Funct. Mater.* **22**, 4763 (2012)
41. D. Jose, A. Datta, *J. Chem. Phys. C* **116**, 24639 (2012)
42. T. Teshome, A. Datta, *ACS Appl. Mater. Inter.* **9**, 34213 (2017)
43. A. Bafekry, *Physica E* **118**, 113850 (2020)
44. H. Sudrajat, S. Hartuti, *Optik* **181**, 1057 (2019)
45. Z.-W. Xiong, L.-H. Cao, *J. Alloy. Compd.* **775**, 100 (2019)
46. S.M. Pratik, C. Chowdhury, R. Bhattacharjee, S. Jahiruddin, A. Datta, *Chem. Phys.* **460**, 101 (2015)
47. A. Bafekry, C. Stampfl, M. Ghergherehchi, S.F. Shayesteh, *Carbon* **157**, 371 (2020)

48. A. Bafekry, S. Farjami Shayesteh, M. Ghergherehchi, F.M. Peeters, J. Appl. Phys. **126**, 144304 (2019)
49. A. Bafekry, C. Stampfl, S. Farjami Shayesteh, F.M. Peeters, Adv. Electron. Mater. **5**, 1900459 (2019)
50. G. Ge, Q. Jing, Z. Yang, Y. Luo, Chin. Phys. Lett. **26**, 083101 (2009)
51. L.J. Shi, Phys. Lett. A. **374**, 1292 (2010)
52. W. Zhang, H.Y. Cho, Z. Zhang, W. Yang, J. Korean Phys. Soc. **69**, 1445 (2016)

Publisher's Note Springer Nature remains neutral with regard to jurisdictional claims in published maps and institutional affiliations.